Talanta 128 (2014) 293–298

Contents lists available at ScienceDirect

Talanta

journal homepage: www.elsevier.com/locate/talanta

Detection of metronidazole and ronidazole from environmental Samples by surface enhanced Raman spectroscopy

Caiqin Han [a,b,c,d,*,1], Jing Chen [b,e,**,1], Xiaomeng Wu [b,e], Yao-wen Huang [b,e], Yiping Zhao [a,b]

[a] Department of Physics and Astronomy, University of Georgia, USA
[b] Nanoscale Science and Engineering Center, University of Georgia, USA
[c] School of Physics and Electronic Engineering, Jiangsu Normal University, China
[d] Jiangsu Province Key Laboratory of Advanced Laser Materials and Devices, China
[e] Department of Food Science and Technology, University of Georgia, USA

ARTICLE INFO

Article history:
Received 21 March 2014
Received in revised form
28 April 2014
Accepted 29 April 2014
Available online 10 May 2014

Keywords:
Surface enhanced Raman spectroscopy
Antibiotics
Nitroimidazoles
Silver nanorods

ABSTRACT

In this study, the surface enhanced Raman spectra (SERS) of two prohibited veterinary drugs, metronidazole (MNZ) and ronidazole (RNZ), have been acquired, and compared to the theoretically calculated spectra using density function theory (DFT). The experimental Raman and SERS spectra of MNZ and RNZ exhibit high resemblance with the DFT calculations. SERS detection of MNZ and RNZ from standard solutions as well as real environmental samples (tap, lake, swamp waters and soil) was performed on highly sensitive and reproducible silver nanorod array substrates. The limits of detection for MNZ and RNZ are 10 and 1 μg/mL in methanol and ultra-pure water, respectively, and 10–50 μg/mL in the environmental samples. The SERS-based method demonstrates its potential as a rapid, simple, and inexpensive means for the onsite screening of banned antibiotics from the aquatic and sediment environments, with minimal requirement for sample pretreatment.

1. Introduction

It is estimated that over 100,000 t of antibiotics are being produced worldwide every year [1]. Although antibiotics have been extensively used to treat infections for decades, their negative impacts on human and animal health as well as on the environment have not been widely recognized until the past two decades [2,3]. The intense use of antibiotics is linked to the emergence and spread of drug resistant or even multi-drug resistant pathogen strains, as in the notorious examples of methicillin-resistant *Staphylococcus aureus* (MRSA), and carbapenem-resistant *Enterobacteriuaceae* (CRE) [4]. The induced antimicrobial resistance can in turn lead to ineffective treatment of potentially deadly infections. In addition to the growing difficulty in disease treatment, some antibiotics have also exhibited in vitro and in vivo carcinogenic properties [5]. Based on these concerns, there is an increasing restriction on the access to antimicrobial drugs through human medicine. Nonetheless, antibiotics are still capable of entering the human diet through transference from animal feed or veterinary drugs to edible tissues of farm animals, fish, and seafood [5]. Moreover, since current household water treatment only aims at removing bacterial and particulate hazards, small, water-soluble antibiotics may still well reside in potable water if the source has been contaminated. Consequently, their use in animals, particularly the use of carcinogenic antibiotics, is also strictly controlled by regulatory bodies.

Metronidazole (MNZ) and ronidazole (RNZ) are two antiprotozoal drugs from the nitromidazole family, which were primarily labeled for the treatment of histomoniasis and trichomoniasis in poultry and hemorrhagic enteritis in pigs, but were later banned by the European Commission and the US food and drug administration (FDA) in food-producing animals due to their suspected genotoxic, carcinogenic, and mutagenic properties [6,7]. Nonetheless, the drugs' side effects on growth promotion and improvement in feed efficiency have led to continued misuse in animals for short-term economic gain. In order to monitor such illegal uses, a number of methods based on liquid (LC) or gas chromatography (GC) coupled with mass spectroscopy (MS) or fluorescence detection have been developed for identifying nitroimidazoles from water, animal tissues, food and feedstuffs, and clinical samples [8–12]. In spite of high sensitivity, these methods have also encountered drawbacks from long assay duration, complicated pre-treatment, low throughput, and high demands on instrumentation. Apparently, the lack of rapid and inexpensive routine

* Correspondence to: 101 Shanghai Road, Tongshan District, Xuzhou, Jiangsu 221116, China.
** Correspondence to: 220 Riverbend Road, Athens, GA 30605, USA.
E-mail addresses: hancq@jsnu.edu.cn (C. Han), jingchen@uga.edu (J. Chen).
[1] Authors of equal contribution.

http://dx.doi.org/10.1016/j.talanta.2014.04.083
0039-9140/

screening for these antibiotics has placed a technical hurdle for effective enforcement of regulations in animals and animal farms. To overcome this challenge, several alternative techniques are being developed. Immunoassays such as enzyme-linked immunosorbent assay (ELISA) have been used for rapid sensing of nitroimidazoles [13]. A surface plasmon resonance (SPR) method was recently developed and validated for screening of nitromidazoles from animal tissues and serum samples [14]. These immunocapture-based methods could achieve excellent detection sensitivity within a relatively short time, but still face some challenges caused by the cross-reactivity and limited availability of drug-specific antibodies.

Like SPR, surface enhanced Raman spectroscopy (SERS) has also been proposed as a sensitive yet simple, rapid, and inexpensive alternative to GC or LC-based techniques. But unlike SPR, SERS can directly reveal the characteristic vibrational modes of the drug molecule, thus it does not rely on the use of antibodies. SERS takes advantage of the enhanced local electromagnetic field due to the specific geometry of the nanostructures of noble metals (Au, Ag and Cu) to amplify the Raman scattering signal by up to 10^6–10^{12} times, and has been used to achieve single molecule detection [15]. A variety of antibiotics have been investigated using SERS or surface enhanced resonance Raman spectroscopy (SERRS), including sulfa drugs (sulfadiazine, sulfamerazine, and sulfamethazine) [16], penicillin and derivatives [17,18], entrofloxacin, ciprofloxacin, chloramphenicol [19], erythromycin [20], nitrofuran antibiotics (furadantin and furaltadone) [21], moxifloxacin [22], and amphotericin and derivatives [23]. Though considered as important targets for antibiotic surveillance, the SERS signature of any nitroimidazole antibiotic is still lacking. Also, since antibiotic standards were detected from aqueous solutions or organic solvents in most of the reported antibiotic SERS studies, but few studies have involved detection from real or spiked samples of environmental, food safety, or clinical relevance, so there is also a need to test the applicability of the SERS technique for real sample detection.

In this study, we have acquired the Raman and SERS spectra of two representative nitroimidazole antibiotics, MNZ and RNZ, and compared the experimental data with theoretical calculation using density function theory (DFT). We have also demonstrated that rapid and facile SERS screening of MNZ and RNZ from tap water, lake water, and swamp water samples and real soil samples could be achieved using a highly uniform silver nanorod substrate prepared by oblique angle deposition.

2. Materials and methods

2.1. Materials and reagents

Metronidazole (MNZ) and Ronidazole (RNZ) were purchased from Sigma Aldrich (St. Louis, MO). Methanol, sulfuric acid, and hydrogen peroxide were obtained from J.T. Baker (Phillipsburgm, NJ). Silver (99.999%) and titanium (99.995%) pellets were obtained from Kurt J. Lesker (Clairton, PA).

2.2. SERS substrate preparation

SERS-active silver nanorod (AgNR) array substrates were fabricated using oblique angle deposition (OAD) in a custom-built electron beam evaporation system as described in our previous studies [24,25]. Briefly, glass slides were cleaned with Piranha solution (80% sulfuric acid, 20% hydrogen peroxide), rinsed with deionized (DI) water, dried with nitrogen gas, and loaded into the deposition chamber. Films of 20 nm of titanium and 200 nm of silver were sequentially deposited onto the glass slides at a normal incidence angle at the rates of 0.2 nm/s and 0.3 nm/s, respectively. In the final step, the substrate surface normal was rotated to an angle of 86° with respect to the vapor incident direction, and silver continued to be deposited at a rate of 0.3 nm/s. The chamber was maintained at a pressure of $<10^{-6}$ Torr throughout the deposition process. The last OAD step yielded a film of aligned nanorods which were ~900 nm in length, ~100 nm in rod diameter, with a tilting angle of approximately 73° with respect to the substrate normal [24,26]. To remove the organic contaminants accumulated during fabrication and storage, before each use for SERS measurements, the as-deposited AgNR substrates were cleaned for 2 min using a custom built inductively-coupled RF plasma chamber, which operated at 30 W under a constant flow of ultra-pure argon with a chamber pressure ~600 mTorr [27].

2.3. Density function theory calculation

In order to identify the corresponding vibrational modes of the obtained Raman peaks, the Gaussian 03 W DFT package was used to calculate the Raman spectra of MNZ and RNZ. The DFT calculations were based on Becke's three-parameter exchange function (B3) [28] with the dynamic correlation function of Lee, Yang, and Parr (LYP) [29]. The molecular geometries of the antibiotics were optimized using the hybrid B3 (exchange) and the LYP (correlation) function (B3LYP) in conjunction with a modest 6–311 g** basis set.

2.4. SERS measurements

All SERS measurements were performed using an Enwave ProRaman-L-785A2 Raman analyzer (Enwave Optronics, Irvine, CA) equipped with a 785 nm diode laser, a spectrometer, and an integrated fiber optic Raman probe for excitation and signal collection through a 10× objective lens. Two microliters of the antibiotic solutions or samples were applied to the substrate surface, allowed to dry under ambient conditions, and SERS spectra were acquired from five randomly selected spots at a laser power of 30 mW and spectral collection time of 10 s.

2.5. MNZ and RNZ standards

To determine the limit of detection (LOD) of SERS measurements, MNZ and RNZ were serially diluted in methanol or DI water, and the dilutions were immediately applied to the surface of the AgNR substrate for SERS measurements. The lower LOD was determined using the 3σ method [30], in which the intensities of characteristic SERS peaks was compared with a threshold value determined by 3× standard deviation of the spectral intensity at a featureless spectral region (1700–1800 cm^{-1}).

2.6. Collection and analysis of environmental samples

Water samples were collected directly from a tap in the laboratory, Lake Herrick in the University of Georgia campus, and from the swamp in the Okefenokee National Wildlife Refuge. MNZ and RNZ were spiked into the water samples at concentrations between 0.01 μg/mL and 1 mg/mL, which were then used for SERS analysis.

Soil was collected from a garden outside the laboratory building after a rainy day, and dried at ambient conditions (the final moisture content was determined to be 0.32%). Aliquots of 1 mL methanol containing different concentrations of MNZ or RNZ were added to 200 mg of soil, mixed on a rocker at 50 rpm for 1 h and then allowed to settle overnight at room temperature (RT). On the second morning, the mixture was Vortexed again and centrifuged at 5000 rpm for 2 min. Two microliters of the supernatant was used for SERS measurements.

2.7. Data analysis

The obtained SERS spectra were analyzed using Origin 8.5 (OriginLab, Northampton, MA). Unless otherwise specified, the raw spectra obtained from the Raman analyzer were used without further processing. Principle component analysis (PCA), partial least square discriminant analysis (PLS-DA), and partial least square regression analysis (PLS) were performed using PLS_Toolbox (Eigenvector, Wenatchee, WA) running under the Matlab 2011b (Mathworks, Denver, CO) environment. The spectra were derivatized to the first order, normalized using the peak height, and mean-centered before PCA, PLS-DA, and PLS analyses.

3. Results and discussion

3.1. SERS spectra of MNZ and RNZ

The major peaks revealed by quantum chemical calculations based on DFT (Supplementary Tables S1 and S2) agree well with the bulk Raman spectra acquired from the antibiotic powder (Fig. 1). Still, several noticeable discrepancies between DFT calculated and experimental spectra are observed, including the disappearance of some DFT-calculated peaks and peak intensity changes, which can be attributed to the DFT's inherent drawbacks [31] as well as the merging effect of adjacent experimental Raman peaks. The Raman spectrum of MNZ obtained in this study is consistent with those acquired in previous reports [32,33], with minor differences in relative peak intensities. This is likely to be caused by the use of different excitation wavelengths. Overall, the DFT and measured bulk Raman spectra of MNZ are quite similar to those of RNZ owing to their similar molecular structures (Supplementary Fig. S1). The most obvious differences are found in the spectral regions near 1100–1170 cm^{-1} and between 1250 and 1380 cm^{-1}, which are attributed to O–H bending, C–H twisting and N–O stretching.

The SERS spectra of MNZ and RNZ (1 mg/mL in methanol) obtained on AgNR substrates further demonstrate the effect of peak merging as fewer peaks are observed (blue curves in Fig. 1). The differences between the Raman and SERS spectra of the antibiotics are expected as the molecules adopt different conformations on the SERS substrate from those in the crystalline powder. Peak shifts could also originate from the interaction between the antibiotic and the silver substrate. On the other hand, like DFT and bulk Raman spectra, the SERS spectra of MNZ and RNZ share high level of resemblance, except for subtle differences near $\Delta\nu = 1380\ cm^{-1}$, which is attributed to O_{10}–N_{12}–O_{11} asymmetrical stretching. Further PCA analysis also indicates that despite the spectral similarity, MNZ and RNZ can be well separated into two distinct clusters in the PCA chart, with their binary mixture grouped as a third cluster in between the two (Supplementary Fig. S2).

3.2. Detection limits of MNZ and RNZ in aqueous solutions

Serial dilutions of MNZ and RNZ prepared in ultra-pure water were used to probe the LODs using SERS (Fig. 2). Though the blank AgNR substrates do not show any significant SERS peaks, the addition of water has led to elevated background and several broad peaks in the spectra (Fig. 2a and b). These peaks are caused by trace amounts of remaining surface contaminants, as water evaporates and causes SERS hot spots to form through the bundling effect of nanorods [34]. At lower concentrations of MNZ and RNZ (below 1–5 μg/mL), these contamination peaks dominate the spectra. But as MNZ and RNZ concentrations increase, characteristic peaks of the antibiotics start to emerge, and displace the peaks from the background. The LODs for MNZ and RNZ in ultra-pure water are thus determined to be 10 and 1 μg/mL, respectively, with the 3σ method. As shown in Fig. 2c and d, the intensity of the MNZ and RNZ peaks experience a noticeable rise in a non-linear fashion as their concentration increases. At ~50–100 μg/mL, the peak intensity of the 1267–1268 cm^{-1} peak reaches a plateau and begins to decrease for RNZ at 1000 μg/mL. Based on the AgNR geometry, the actual surface area of the spread 2-μL sample spot is approximately $3.75 \times 10^{14}\ nm^2$, and the number of molecules within the spot is 6.02×10^{14}–7.03×10^{14}. Therefore, the average surface coverage of the antibiotics is between 1.6 and 1.9 molecules/nm^2, which implies that the surface coverage of the antibiotics is very close to what is sufficient to form a monolayer if a uniform coverage is assumed, and the surface will be packed by the antibiotic molecules at ~100 μg/mL. Since previous studies have reported a reduction in SERS intensity due to adsorbate excited state quenching [35], it is not surprising that the peak intensities of RNZ decline at 1000 μg/mL.

Conventionally, the LOD of a detection method refers to the lowest detectable concentration of the bulk analyte solution. It is influenced by the area on the substrate which liquid samples spread into, the area of the incident laser spot, and the true mass sensitivity of the sensing platform. Taking these factors into consideration, the true mass sensitivity of the SERS platform can be expressed as the lowest amounts of MNZ and RNZ that could be detected, i.e., lowest detectable mass (LDM) of the analytes, which

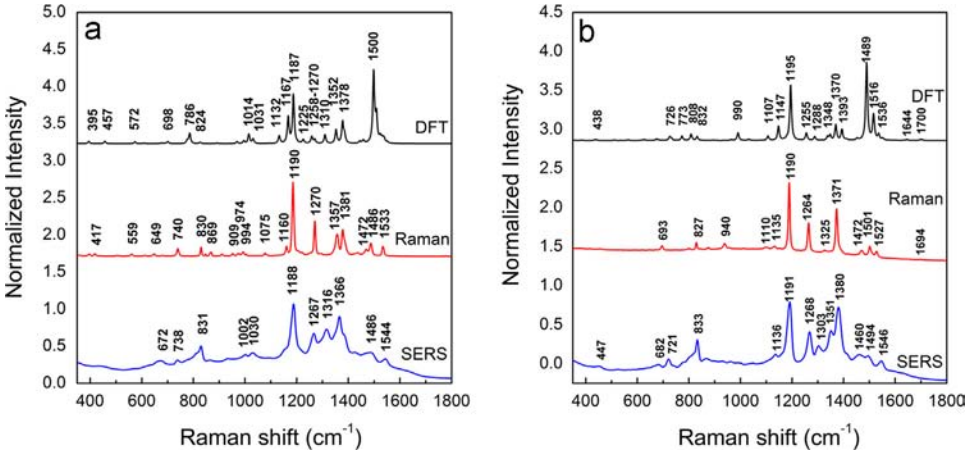

Fig. 1. The Raman spectra calculated by DFT (black) and corresponding bulk Raman (red) and SERS (blue) spectra of (a) MNZ and (b) RNZ. Spectra are normalized to the most intensive peaks and offset for clarification.

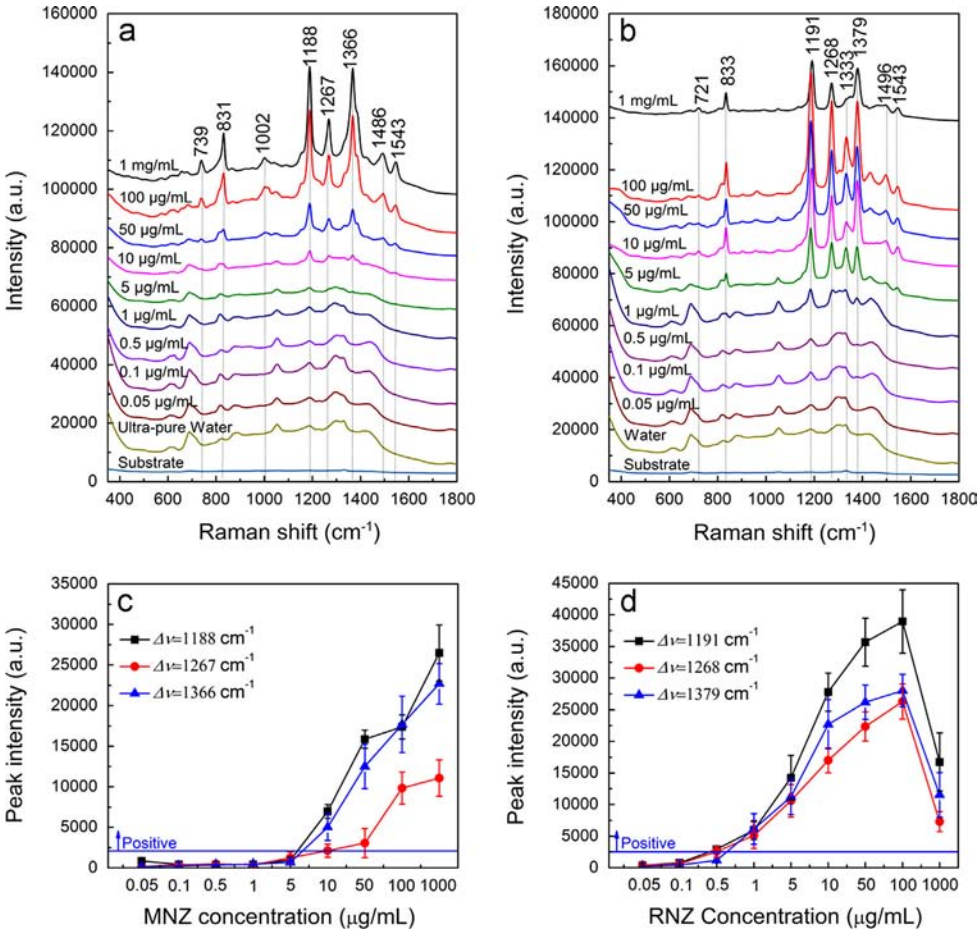

Fig. 2. SERS spectra of (a) MNZ and (b) RNZ at different concentrations in ultra-pure water and characteristic peak intensities of (c) MNZ and (d) RNZ. Spectra are offset for clarification. The blue lines in (c) and (d) indicate the threshold 3σ values used to determine positive or negative responses. (For interpretation of the references to color in this figure legend, the reader is referred to the web version of this article.)

can be calculated by

$$\mathrm{LDM} = \frac{CVA}{A_0}, \tag{1}$$

where C is the concentration of MNZ or RNZ, V is the volume of solution ($V=2\ \mu L$), A is the area of the Raman laser spot ($A=0.0143\ mm^2$), and A_0 is the area of the circular spot which the sample has spread into ($A_0=78.5\ mm^2$). The LDMs are estimated to be 10^{-12} g for MNZ and 2×10^{-14} g for RNZ, demonstrating high inherent sensitivity of the SERS method. The sensitivity of the current SERS assay matches with previous reports on other antibiotics which utilized silver or gold nanoparticles as SERS active substrates (1.5–5 μg/mL) [22,36]. Since the AgNR substrate is noted for its superior signal reproducibility compared with nanoparticle substrates [24], it may be better suited for real-world applications.

3.3. Detection of MNZ and RNZ in spiked water samples

Aquatic systems are an important source for human exposure to antibiotics. Though treatment of sewage water from hospitals or pharmaceutical plants is strictly enforced in many countries, contamination from other sources is largely unpredictable [37]. Hence quick testing for antibiotic residues in the water systems is desirable to ensure food safety and animal health. Here we chose three types of water sources, i.e., tap drinking water, lake water, and swamp water to evaluate the effectiveness of the SERS-based test. The water samples were subject to no further treatment after sampling except spiking of antibiotics, and the spiked samples were directly measured on the SERS substrates. As shown in Fig. 3, water from tap, fresh water lake, and swamp exhibits distinct spectral features. The SERS spectrum of tap water is a broad hum across the region between $\Delta\nu=600$–$1800\ cm^{-1}$ with no apparent peaks. Comparing with the spectrum of ultra-pure water (Fig. 2), the featureless spectrum of tap water clearly suggests that tap water is somehow able to mask the spectral contribution from surface contaminant residues. Interestingly, as the antibiotic concentration increases, contamination peaks at $\Delta\nu=690$, 818, 881, 1052, 1187, 1296–1330, and $1432\ cm^{-1}$ which are seen in ultra-pure water begin to reemerge (Supplementary Fig. S3). Though the exact mechanisms of this "peak scavenging" effect are not within the scope of this study, we speculate that it involves the AgNRs' tendency to be oxidized by chlorine in tap water that has led to a loss in SERS activity of the substrate. In the presence of higher concentrations of antibiotics, however, the added molecules protect the AgNRs by competing with adsorption sites on the silver surface, even though the SERS signal of antibiotics themselves is still too weak to reach the detection threshold. The spectrum of lake water (Supplementary Fig. S4), on the other hand, shows similar peaks to that of ultra-pure water, with additional peaks at $\Delta\nu=1160$ and $1620\ cm^{-1}$, which may be contributed by trace amount of humic acids that have diffused into surface water from the lake sediment [36]. The swamp water spectrum displays two broad peaks near $\Delta\nu=1320$ and $1590\ cm^{-1}$, but these two peaks are likely to result from a series of convoluted peaks, as the composition of wetland water is expected to be much more complex due to biological diversity.

Despite complex compositions of the lake and swamp water compared to ultra-pure and tap water, only small interference from these constituents was observed in the obtained SERS spectra for MNZ and RNZ detection. The LODs of MNZ in tap, lake, and swamp water are determined to be 10, 50, and 50 μg/mL, respectively, and the LODs of RNZ are found to be 10 μg/mL in all three cases (see Supplementary Fig. S5 for spectral and peak intensity analyses). The interference from impurities in the lake/swamp water samples has led to an LOD for MNZ roughly ten times higher than in pure water, while the LODs for RNZ remain unaffected. This suggests that during competitive adsorption on the substrate, RNZ has a slight advantage over MNZ, possibly as a result of its carboxyl and end-amino groups, which have stronger binding tendency to silver. In fact, this also explains the lower LOD of RNZ observed in ultra-pure water.

PLS-DA prediction models have also been established to evaluate the detection accuracy in water samples. Except for one positive RNZ data point (10 μg/mL in swamp water) which is misclassified as negative, all other measurements of MNZ/RNZ in tap, lake, and swamp water samples were accurately classified using the prediction model (see Supplementary Figs. S6–S8 for more discussions on PLS-DA analysis). In addition, PLS regression also reveals good linear correlation between the spectral response and the true concentration of the samples (R^2=0.81–0.99; see Supplementary Figs. S10–S13 for more details).

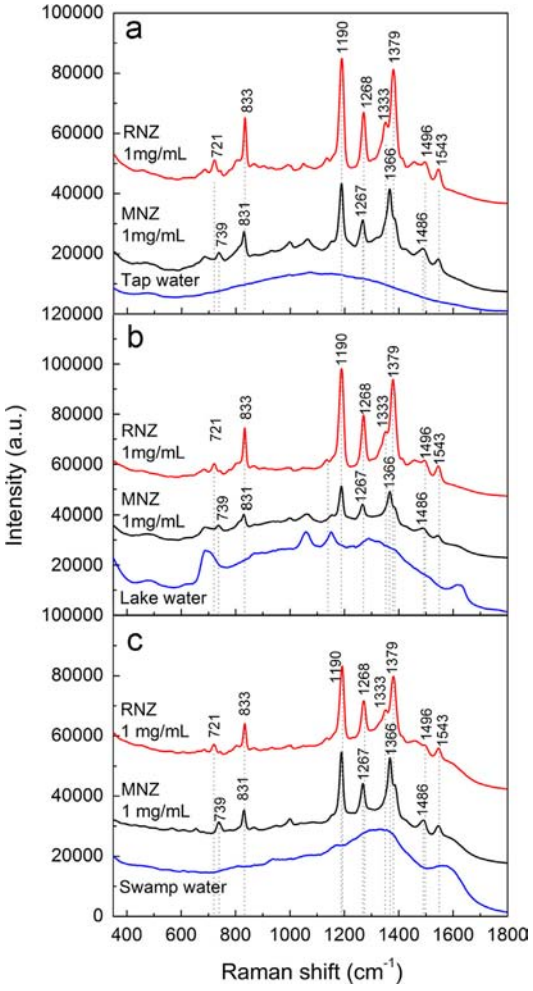

Fig. 3. SERS spectra of spiked MNZ and RNZ in (a) tap water (b) lake water and (c) swamp water samples. Spectra are offset for clarification.

3.4. Detection of MNZ and RNZ in the presence of soil

Besides aquatic systems, antibiotic residues may also be found in the sediments, particularly in ground soil, dirt, or mud in poultry, cattle, and pig farms as a result of carryover from adulterated animal feed. Antibiotics or their metabolites can also enter soil with fertilized manure using feces from dosed animals or from contaminated sewage sludge [1]. It is therefore desired to detect banned antibiotics such as MNZ and RNZ for monitoring their use in animals. To mimic this type of environment samples and to further evaluate detection ability of the proposed method, we obtained top soil from an outdoor garden and spiked with different amounts of MNZ and RNZ for testing with SERS. After overnight incubation, antibiotic molecules have presumably reached equilibrium between the methanol solution and the surface of soil particles, and some minerals and organic matters in soil have diffused into the methanol phase. Vortexing this mixture forces the antibiotic molecules adsorbed on the soil particle to reenter into the liquid, and more soil constituents are likely to dissolve. Hence after overnight equilibration and subsequent mixing, the diffusion of soil introduces a new peak to the SERS spectrum of blank soil sample at $\Delta\nu$=1610 cm^{-1} (Fig. 4, also see spectrum of ultra-pure water in Fig. 2 for comparison), which

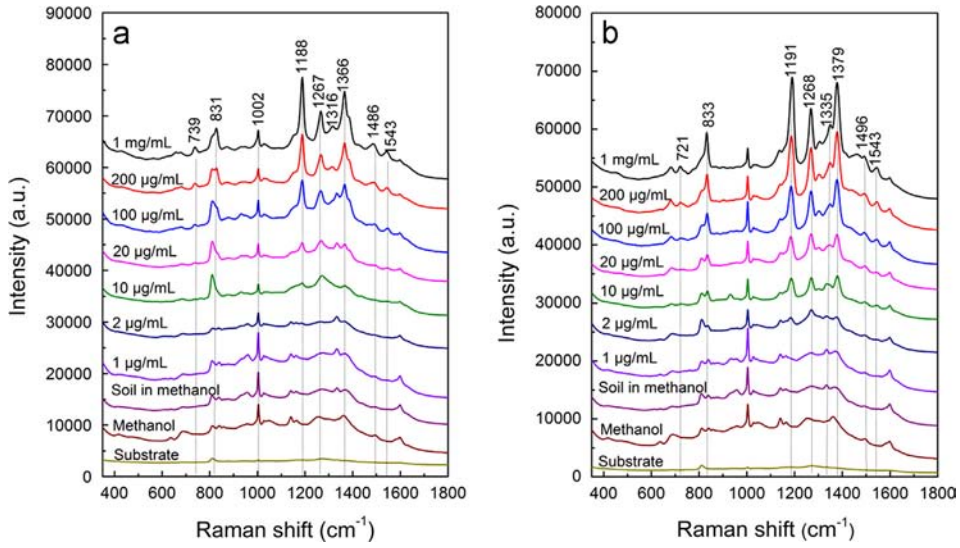

Fig. 4. SERS spectra of (a) MNZ and (b) RNZ in spiked soil samples. Spectra have been offset for clarification.

may be attributed to humus or humic acids, a major organic constituent found in soil [36]. Not surprisingly, this also coincides with the spectrum of lake water, indicating that part of the lake spectrum may originate from diffusion of soil sediments. Nevertheless, the background spectral features of soil do not appear to significantly affect the detection of antibiotics. As Fig. 4 shows, when the antibiotics are mixed with soil, typical MNZ and RNZ peaks begin to emerge and peak intensities continue to increase with increasing antibiotic concentrations. Finally, the LODs are found to be 10 and 2 μg/mL for MNZ and RNZ, respectively, only marginally higher than those observed with aqueous or methanol standard solutions, which is further confirmed by the PLS-DA prediction model (Supplementary Fig. S9). This means that the interference from soil components is negligible for SERS detection.

The ability to detect MNZ and RNZ in the presence of soil demonstrates that the current SERS detection platform has a potential of handling complex environmental samples such as soil, with relatively simple sample preparation and no requirement for cleanup before detection. This could be advantageous considering that sample preparation is still a major limitation in conventional antibiotic detection techniques (e.g., LC–MS).

4. Conclusion

In this study we have calculated the Raman spectra of two prohibited antibiotic drugs, MNZ and RNZ by DFT. The Raman and SERS spectra of MNZ and RNZ were acquired for the first time, which show high resemblance with DFT-calculated spectra. SERS measurements based on highly uniform AgNR array substrates were conducted to detect MNZ and RNZ from both standard solutions and real aquatic and soil samples. The SERS-based detection demonstrates high inherent sensitivity (as low as 10^{-12} g MNZ and 2×10^{-14} g RNZ could be detected) and LODs at lower ppm levels in aqueous solutions. Furthermore, a comparison in the spectra and LODs between standard solutions and real environmental samples reveals that the detecting ability appears to be minimally affected by matrix effect from the samples. This implies that complex and time-consuming procedures used in traditional techniques may be circumvented or simplified by the SERS-based method, which may further be developed for rapid onsite screening of antibiotic contamination. Admittedly, in spite of the simplicity and rapidity of SERS, the detection limits of MNZ and RNZ in terms of bulk concentrations are still not satisfactory in comparison to the legislative standards or mainstream techniques such as LC–MS, with LODs as low as sub-μg/L from water samples [9]. This is primarily because as a surface technique, SERS requires the analytes to be spread onto the sensing surface before detection, which means only the molecules within the Raman laser spot can be detected while the majority of the sample is wasted (roughly only one out of 5500 analyte molecules on the sensing surface is probed by comparing the area of the laser spot with the sample spreading area). But for LC–MS, a bulk volume of samples has been running through the column. Nevertheless, the detection efficiency of SERS can be significantly improved with further modification of the platform. For instance, SERS can be used in conjunction with facile electrochemistry techniques to concentrate analytes on the exact sensing area [38]. For more complicated samples, a simple pre-detection chromatographic separation directly on the sensing chip could also be helpful [39].

Acknowledgments

This research was founded by National Science Foundation under contract number CBET-1064228. The authors thank Dr. Xibo Li for setting up DFT calculations, and Mr. Layne Bradley for proofreading the manuscript. C.H. would like to thank the National Natural Science Foundation of China (Grant no. 21375051) and the Priority Academic Program Development of Jiangsu Higher Education Institutions for their generous financial support of her research conducted at the University of Georgia. J.C. would like to thank UGA College of Agricultural and Environmental Sciences Experimental Station for their generous financial support.

Appendix A. Supplementary information

Supplementary data associated with this article can be found in the online version at http://dx.doi.org/10.1016/j.talanta.2014.04.083.

References

[1] K. Kummerer, Chemosphere 75 (2009) 417–434.
[2] G.G. Khachatourians, Can. Med. Assoc. J. 159 (1998) 1129–1136.
[3] C. Verraes, S. Van Boxstael, E. Van Meervenne, E. Van Coillie, P. Butaye, B. Catry, M.-A. de Schaetzen, X. Van Huffel, H. Imberechts, K. Dierick, G. Daube, C. Saegerman, J. De Block, J. Dewulf, L. Herman, Int. J. Environ. Res. Public Health 10 (2013) 2643–2669.
[4] J. Ho, Curr. Opin. Infect. Dis. 23 (2010) 546–553.
[5] J.L. Davis, G.W. Smith, R.F. Baynes, L.A. Tell, A.I. Webb, J.E. Riviere, J. Am. Vet. Med. A 235 (2009) 528–534.
[6] F.J. Roe, Surgery 93 (1983) 158–164.
[7] C.E. Voogd, J.J. Van Der Stel, J.J.J.A.A. Jacobs, Mutat. Res. 26 (1974) 483–490.
[8] C. Ho, D.W.M. Sin, K.M. Wong, H.P.O. Tang, Anal. Chim. Acta 530 (2005) 23–31.
[9] L.F. Capitan-Vallvey, A. Ariza, R. Checa, N. Navas, J. Chromatog. A 978 (2002) 243–248.
[10] J. Zhou, J. Shen, X. Xue, J. Zhao, Y. Li, J. Zhang, S. Zhang, J. AOAC Int. 90 (2007) 872–878.
[11] C. Mahugo-Santana, Z. Sosa-Ferrera, M.E. Torres-Padrón, J.J. Santana-Rodríguez, Anal. Chim. Acta 665 (2010) 113–122.
[12] L.F. Capitan-Vallvey, A. Ariza, R. Checa, N. Navas, Chromatographia 65 (2007) 283–290.
[13] A.-C. Huet, L. Mortier, E. Daeseleire, T. Fodey, C. Elliott, P. Delahaut, Anal. Chim. Acta 534 (2005) 157–162.
[14] C.S. Thompson, I.M. Traynor, T.L. Fodey, S.R.H. Crooks, Anal. Chim. Acta 637 (2009) 259–264.
[15] K. Kneipp, H. Kneipp, S. Abdali, R.W. Berg, H. Bohr, Spectrosc.-Int. J. 18 (2004) 433–440.
[16] W.S. Sutherland, J.J. Laserna, M.J. Angebranndt, J.D. Winefordner, Anal. Chem. 62 (1990) 689–693.
[17] V. Reipa, J.J. Horvath, Appl. Spectrosc. 46 (1992) 1009–1013.
[18] S.J. Clarke, R.E. Littleford, W.E. Smith, R. Goodacre, Analyst 130 (2005) 1019–1026.
[19] L.L. He, M.S. Lin, H. Li, N.J. Kim, J. Raman. Spectrosc. 41 (2010) 739–744.
[20] A. Marz, S. Trupp, P. Rosch, G.J. Mohr, J. Popp, Anal. Bioanal. Chem. 402 (2012) 2625–2631.
[21] W. Xie, C. Han, J.B. Hou, F. Wang, Y. Qian, J.Y. Xi, J. Sep. Sci. 35 (2012) 3447–3454.
[22] M.B. Mamian-Lopez, R.J. Poppi, Anal. Bioanal. Chem. 405 (2013) 7671–7677.
[23] Y. Ridente, J. Aubard, J. Bolard, Biospectroscopy 2 (1996) 1–8.
[24] Y.J. Liu, H.Y. Chu, Y.P. Zhao, J. Phys. Chem. C 114 (2010) 8176–8183.
[25] J.X. Fu, A. Collins, Y.P. Zhao, J. Phys. Chem. C 112 (2008) 16784–16791.
[26] J.D. Driskell, S. Shanmukh, Y. Liu, S.B. Chaney, X.J. Tang, Y.P. Zhao, R.A. Dluhy, J. Phys. Chem. C 112 (2008) 895–901.
[27] P. Negri, N.E. Marotta, L.A. Bottomley, R.A. Dluhy, Appl. Spectrosc. 65 (2011) 66–74.
[28] A.D. Becke, J. Chem. Phys. 98 (1993) 5648.
[29] C. Lee, W. Yang, R.G. Parr, Phys. Rev. B.: Condens. Matter 37 (1988) 785–789.
[30] W.B. Knighton, E.P. Grimsrud, Anal. Chem. 55 (1983) 713–718.
[31] X.M. Wu, S.M. Gao, J.S. Wang, H.Y. Wang, Y.W. Huang, Y.P. Zhao, Analyst 137 (2012) 4226–4234.
[32] L. Xu, K. Ding, X. Guo, C. Wang, H. Juying, J. Capital Univ. Med. Sci. 27 (2006) 785–787.
[33] Z.-G. Ling, Y.-L. Tang, T. Li, Y.-P. Li, D. Jian-Bing, J. Atom. Mol. Phys. 30 (2013) 553–558.
[34] J.L. Abell, J.D. Driskell, Y. Zhao, Chem. Comm. 50 (2014) 106–108.
[35] E. Zeman, K. Carron, G. Schatz, R. Van Duyne, J. Chem. Phys. 87 (1987) 4189–4200.
[36] T. Wang, F.-p. Zhong, Y.-h. Yang, D.-h. Zhang, Spectrosc. Lett. 29 (1996) 1449–1458.
[37] R. Lindberg, P.Å. Jarnheimer, B. Olsen, M. Johansson, M. Tysklind, Chemosphere 57 (2004) 1479–1488.
[38] Y.T. Li, L.L. Qu, D.W. Li, Q.X. Song, F. Fathi, Y.T. Long, Biosens. Bioelectron. 43 (2013) 94–100.
[39] J. Chen, J. Abell, Y.-W. Huang, Y. Zhao, Lab Chip 12 (2012) 3096–3102.